CHEMISTRY
AN ASIAN JOURNAL
ACES
FULL PAPER

DOI: 10.1002/asia.201300501

Conjugated Polyelectrolytes with Aggregation-Enhanced Emission Characteristics: Synthesis and their Biological Applications

Rongrong Hu,[a, b] Ruquan Ye,[b] Jacky W. Y. Lam,[a, b] Min Li,[b] Chris W. T. Leung,[b] and Ben Zhong Tang*[a, b, c]

Dedicated to Professor Chunli Bai on the occasion of his 60th birthday

Abstract: Conjugated polyelectrolytes are promising candidates for the construction of fluorescent bioprobes. In this study, a series of water-soluble fluorescent polyelectrolytes have been designed and synthesized by means of the quaternization of their tetraphenylethene-containing polyyne precursors. The polyynes can be facilely prepared through Hay–Glaser polycoupling in high yields (up to 99%) with high molecular weights (up to 38900). All the polymers exhibit a phenomenon of aggregation-induced or -enhanced emission. The fluorimetric titrations of biomolecules such as heparin, calf thymus DNA, RNA, bovine serum albumin, and human serum albumin to buffer solutions of the polyelectrolytes suggest that they are promising fluorescent bioprobes with high sensitivity and fast response. The emission intensity of the polyelectrolytes is enhanced by up to sevenfold upon binding with biomolecules through electrostatic and hydrophobic cooperative interactions. The polyelectrolytes can also serve as fluorescent visualizers for intracellular imaging with good biocompatibility and low autofluorescence interference.

Keywords: aggregation · electrolytes · fluorescent probes · imaging agents · polymers

Introduction

The development of new technologies for the detection of biomolecules has attracted much academic and industrial interest because of the rapidly increasing demand for genetic analysis, clinical diagnosis, biowarfare, environmental analysis, and homeland defense.[1] Among various methods such as the traditionally used colorimetric techniques[2] for protein quantitation, fluorescence-based probes have received special attention owing to their high sensitivity, selectivity, and rapidity.[3] Although inorganic quantum dots and fluorescent nanoparticles offer improved photostability and high luminescence quantum efficiency, they introduce new problems such as difficult synthesis, limited variety, and high cytotoxicity.[4] Organic dyes, on the other hand, provide the opportunity for chemical-structure modification, thus enabling fine-tuning of their photophysical properties by systematic structural variation.[5] Although much progress has been made in this field, major challenges that limit the practical high-tech applications of fluorescent bioprobes, such as poor solubility in aqueous media, poor stability under ambient conditions, insufficient biocompatibility, expensive prices due to painstaking syntheses, and so on, remain to be solved.[6] The development of readily accessible and environmentally stable bioprobes with high sensitivity and selectivity is thus in urgent demand.

Water-soluble fluorescent conjugated polyelectrolytes (CPEs) have long been recognized as an important class of materials owing to the unique combination of the optoelectronic properties of the conjugated polymers and the potential electrostatic interactions between the polyelectrolytes and the analytes. They afford a unique platform for the development of highly sensitive fluorescence-based sensors with fast response for biological targets and are of great academic and technological importance.[7] Most conjugated polyelectrolyte-based biosensors rely on the fluorescence-intensity change upon binding with the bioanalyte.[8] The analyte-induced aggregation of polymer backbones through electrostatic and hydrophobic cooperative interactions was the most widely adopted sensing mechanism for CPEs.[9] In this process, multiple charges and hydrophobic cavities in

[a] Dr. R. Hu, Dr. J. W. Y. Lam, Prof. B. Zhong Tang
The Hong Kong University of Science & Technology (HKUST)
Shenzhen Research Institute
No. 9 Yuexing 1st RD, South Area, Hi-tech Park
Nanshan, Shenzhen, 518057 (China)
Fax: (+85) 2-23581594
E-mail: tangbenz@ust.hk

[b] Dr. R. Hu, R. Ye, Dr. J. W. Y. Lam, M. Li, C. W. T. Leung, Prof. B. Zhong Tang
Department of Chemistry
Institute of Molecular Functional Materials
and Division of Biomedical Engineering, HKUST
Clear Water Bay, Kowloon, Hong Kong (P.R. China)

[c] Prof. B. Zhong Tang
Guangdong Innovative Research Team
SCUT-HKUST Joint Research Laboratory
State Key Laboratory of Luminescent Materials and Devices
South China University of Technology (SCUT)
Guang Zhou 51064 (P.R. China)

Supporting information for this article is available on the WWW under http://dx.doi.org/10.1002/asia.201300501.

the biomolecules facilitate the formation of aggregates, thereby resulting in a remarkable fluorescence change of the aqueous solution and thus realizing analyte detection. Typical CPE-based fluorescence assays allow detection of the target analytes in the nanomolar[10] or even picomolar[11] concentration ranges. This is a major advantage of CPEs, considering that the detection sensitivity is one of the most important aspects in biosensor development with the ultimate goal being the trace detection of genes or proteins in biological fluids.

Poly(*p*-phenylenevinylene)s, poly(thiophene)s, poly(phenylene ethynylene)s, poly(*p*-phenylene)s, and polyfluorenes are widely used as conjugated polyelectrolytes for the construction of bioprobes.[12] However, these CPEs generally do not exist as isolated chains and form simple solutions in pure water. Instead, they tend to form aggregates in aqueous buffers.[13] The aggregation of the polymer chains favors the formation of detrimental species such as excimers and exciplexes and causes nonradiative relaxation of the excited states. Such an aggregation-caused quenching (ACQ) effect of light emission in the aggregated state adversely affects their emission properties and has consequently hampered their application as bioprobes.[14] Recently, we and other groups observed a phenomenon of aggregation-induced emission (AIE) that is the exact opposite to the ACQ effect: a series of propeller-shaped molecules such as tetraphenylethenes (TPEs), siloles, butadienes, pyrans, and fulvenes are nonemissive in the solution state but become highly luminescent in the aggregated state.[15] Through a series of designed experiments and theoretical calculations, we proposed the restriction of intramolecular rotation as the main cause for the AIE effect. Decorating AIE-active compounds with ionic or polar functional groups renders the dyes water-soluble, which means they can be utilized as fluorescent probes for bioanalyses.[16] In fact, we and many research groups have succeeded in utilizing TPE-based AIE luminogens for nucleic acid detection, enzymatic activity assay, and metallic ion tracing.[17] Such promising results prompted us to solve the notorious ACQ problem of current CPE-based bioprobes by utilizing AIE-active CPEs and explore their applications in bioanalyses further.

In this study, we designed and synthesized a series of TPE-containing conjugated polyelectrolytes and investigated their utilities as fluorescent bioprobes for the detection of heparin, nucleic acids (ctDNA and RNA), and proteins (BSA and HSA). The fluorescence of the TPE-containing CPEs in aqueous buffer solutions was greatly enhanced upon binding to the biomacromolecules by means of electrostatic attraction and hydrophobic interaction on account of their multiple positive charges and the hydrophobic nature of their polymer backbones.

Results and Discussion

Polymer Synthesis

Polyelectrolytes **P1**–**P4** were synthesized according to the reaction routes shown in Schemes 1 and 2. The palladium-catalyzed Sonogashira coupling reaction of 4,4′-dibromobenzophenone (**10**) with trimethylsilylacetylene (TMSA) furnished product **8**. Treatment of 4,4′-dihydroxybenzophenone (**11**) with an excess amount of 1,2-dibromoethane afforded **9**, which then underwent a McMurry coupling reaction with **8** to generate intermediate **7**. The trimethylsilyl groups of **7** were cleaved under basic conditions, thereby furnishing the desirable TPE-containing monomer **5**. Hay–Glaser polycoupling of **5** at 50 °C in the presence of CuCl and *N*,*N*,*N*′,*N*′,-

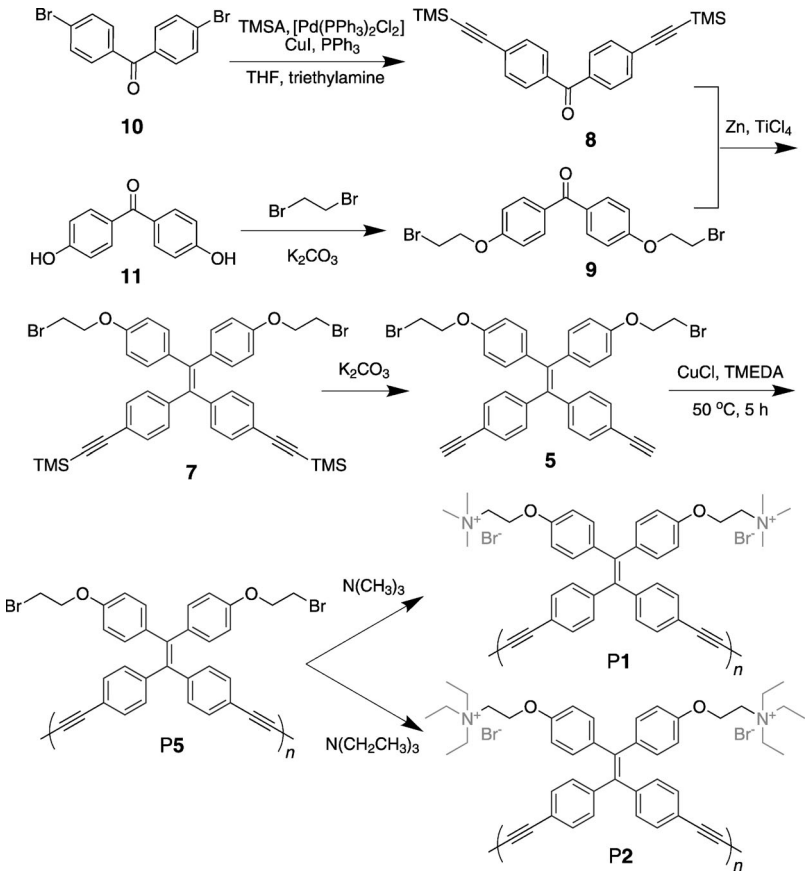

Scheme 1. Synthetic routes to polymers P**1** and P**2**.

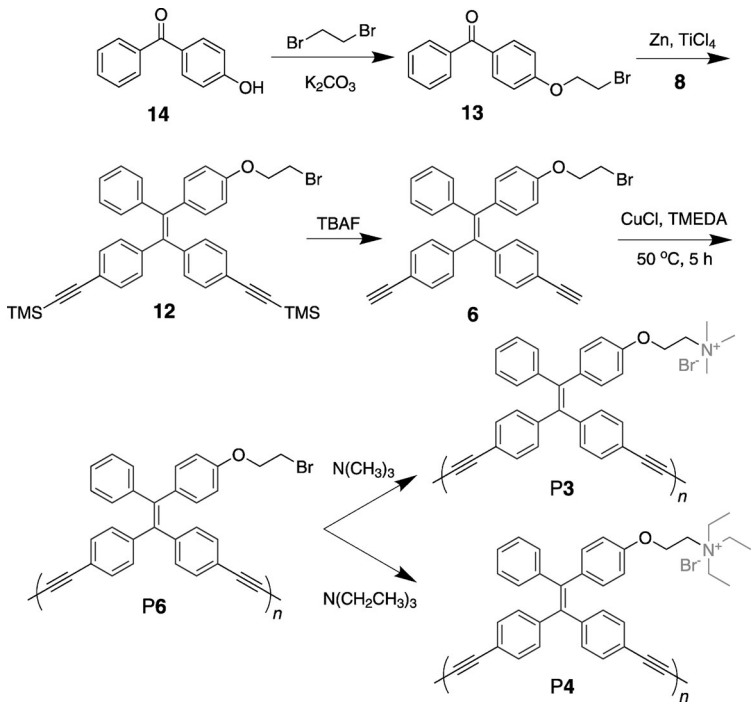

Scheme 2. Synthetic routes to polymers P**3** and P**4** (TBAF: tetrabutylammonium fluoride).

tetramethylethenediamine (TMEDA) in 1,2-dichlorobenzene (*o*-DCB) for 5 h produced P**5** with a weight-average molecular weight (M_w) of 38900 in nearly quantitative yield. Treatment of P**5** with an excess amount of trimethylamine or triethylamine furnished polyelectrolytes P**1** and P**2** in high yields. Similarly, TPE-containing polyelectrolytes P**3** and P**4** with one trialkylammonium group on each repeating unit were successfully obtained by similar synthetic pathways by using monohydroxybenzophenone (**14**) instead of **11** as the starting material.

Structural Characterization

All the intermediates and products were characterized by IR and NMR spectroscopies and gave satisfactory analytical data that corresponded to their expected molecular structures (see the Experimental Section for details). Their high-resolution mass spectra gave M^+ peaks at m/z 624.0311 (624.0300, calcd for **5**) and 502.0933 (502.0932, calcd for **6**), thereby confirming the formation of the expected monomers (see the Supporting Information).

The IR spectra of **5** and P**5** are given in the Supporting Information as an example. The strong absorption bands observed at 3290 and 2105 cm^{-1} in **5** are associated with its ≡C–H and C≡C stretching vibrations, respectively. These bands are absent in the spectra of P**5**, and new absorption peaks related to C≡C–C≡C stretching vibrations emerge at 2202 and 2141 cm^{-1}, thereby suggesting that all the triple bonds of **5** have been consumed by the polycoupling reaction. Similarly, the spectrum of P**6** shows no ≡C–H and C≡C stretching vibrations of **6** at 3290 and 2109 cm^{-1}, and new absorption peaks related to the stretching of the diyne functionality are observed at 2205 and 2143 cm^{-1} (see the Supporting Information). The IR spectra of P**1**–P**4** largely resemble those of P**5** and P**6**, except for the new peaks associated with aliphatic C–H stretching vibrations at 2872–2678 cm^{-1} (see the Supporting Information).

Similar results are obtained from the ^1H NMR spectroscopic analyses. The singlet peak at $\delta = 3.05$ ppm in the spectrum of **5** originates from the absorption of its terminal acetylene proton, which weakens substantially in the spectrum of P**5** (see the Supporting Information). The same trend was observed in the spectra of **6** and P**6**: the peak at $\delta = 3.06$ ppm on account of the terminal acetylene proton resonance of **6** disappears in the spectrum of P**6**, which is indicative of the complete consumption of the triple bond by the polymerization. Meanwhile, the absorption peaks of P**6** are significantly broadened relative to those of **6** owing to its polymeric nature (see the Supporting Information). Strong peaks due to the absorptions of the methyl and ethyl groups of the ammonium salt moieties are observed in the spectra of P**1** and P**2** at $\delta = 3.33$–3.27 and 3.46 and 1.26 ppm, respectively. These findings verify their polyelectrolyte structures and suggest that the quaternization reaction proceeds to a great extent.

Solubility

CPEs P**1**–P**4** dissolve completely or partially in water, whereas P**5** and P**6** possess good solubility in common organic solvents such as toluene, dichloromethane, chloroform, THF, and so on. On the other hand, all the polymers are soluble in DMSO. CPEs with trimethylammonium groups (P**1** and P**3**) show better water solubility than those with triethylammonium functionalities (P**2** and P**4**). The magnitude of charge in each repeating unit also affects the water solubility. After taking into the account all these aspects, P**1** possesses the best water solubility and can facilely dissolve in water or aqueous buffer.

Photophysical Properties

The absorption spectra of the polymers in dilute solutions (10 μM) are shown in Figure 1. The post-polymerization slightly alters the ground-state electronic transition, and the absorption maximum of P**1** and P**2** as well as their precursor

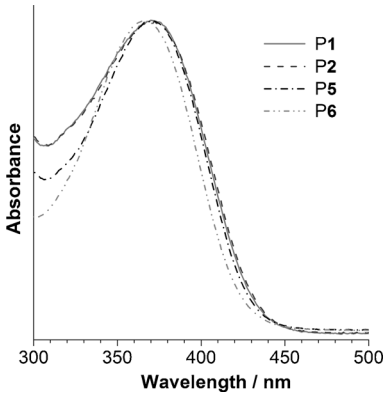

Figure 1. Normalized absorption spectra of P**1** and P**2** in DMSO, and P**5** and P**6** in THF. Concentration: 10 μM.

P**5** is located at 372 nm. The absorption of P**6** is blueshifted 6 nm from that of P**5**, thereby revealing that the bromoethoxy group contributes to the conjugation of the polymer.

Studies of the photoluminescence (PL) properties of P**5** and P**6** reveal that they exhibit the typical phenomenon of aggregation-enhanced emission (AEE) or AIE. The iconic impression of the AIE/AEE features of P**5** and P**6** are given by their fluorescent photographs in THF and THF/water mixtures, which are shown in Figures 2A and 3A. Whereas the solution of P**5** in THF emits weak yellow light, addition of water, a nonsolvent of the polymer, into the solution induces the polymer chains to aggregate and enhance its emission intensity. The emission remained weak until 30 vol% water was added, after which it started to increase. The solution of P**6** in THF, however, emitted no light under UV irradiation, whereas an intense yellow emission was observed

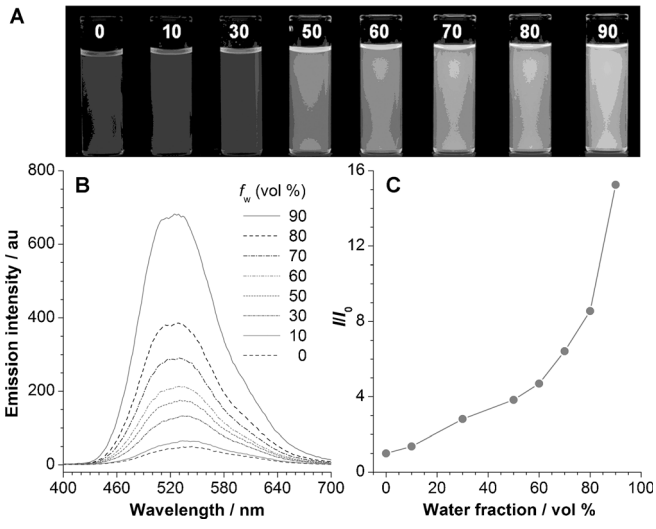

Figure 2. A) Photographs of P**5** in THF/water mixtures with different water fractions (f_w) taken under 365 nm UV irradiation from a hand-held UV lamp. B) Emission spectra of P**5** in THF/water mixtures with different f_w values. C) Plot of relative PL intensity (I/I_0) versus the composition of the aqueous mixture of P**5**. Solution concentration: 10 μM; excitation wavelength: 372 nm.

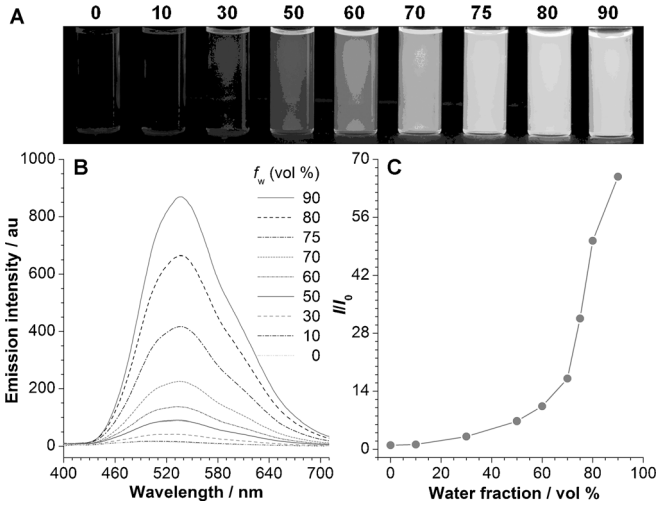

Figure 3. A) Photographs of P**6** in THF/water mixtures with different water fractions (f_w) taken under 365 nm UV irradiation from a hand-held UV lamp. B) Emission spectra of P**6** in THF/water mixtures with different f_w values. C) Plot of relative PL intensity (I/I_0) versus the composition of the aqueous mixture of P**6**. Solution concentration: 10 μM; excitation wavelength: 366 nm.

when its chains aggregated in the presence of a large amount of water (≥70 vol%).

To have a quantitative picture, the emission behaviors of P**5** and P**6** in THF and THF/water mixtures were investigated with a PL spectrophotometer. Compound P**5** emits faintly at 536 nm in THF (Figure 2). Addition of water increases the emission intensity, progressively accompanied by a blueshift in the emission maximum. From the isolated species in THF to aggregates in a 90% aqueous mixture, the emission intensity rises 15-fold, whereas the emission maximum blueshifts by 11 nm. Unlike P**5**, no emission is detected from the solution of P**6** in THF. When its chains aggregate in the presence of water, an emission peak emerges at 536 nm, the intensity of which increases gradually with increasing water content in the THF/water mixture. In 90% aqueous mixture, the intensity is 65-fold higher than that in THF. The steric effect of the bromoethoxy groups in P**5** might inhibit the free rotation of the TPE units, thus rendering the polymer emissive in solution. It also makes the polymer adopt a more twisted structure, and a bluer emission is detected in the aggregated state than in that of P**6**.

Fluorimetric Heparin Titration

Heparin is a highly sulfated glycosaminoglycan with an average molecular weight of approximately 15000 Da; it is widely used as an injectable anticoagulant.[18] Among all known biological molecules, heparin has the highest negative charge density. The anticoagulant activity of heparin is due to its interaction with the proteins involved in the blood-clotting cascade. It is thus crucial to monitor the heparin level. With this in mind, fluorescence titrations of heparin using P**1** and P**2** in aqueous solutions were carried out. The polymers were first dissolved in DMSO to give solu-

tions with a concentration of 10^{-3} M, and then they were diluted to 5 μM with water. As shown in Figure 4, the aqueous solution of P**1** shows an emission peak at 520 nm. When a small amount of heparin solution was added, the emission

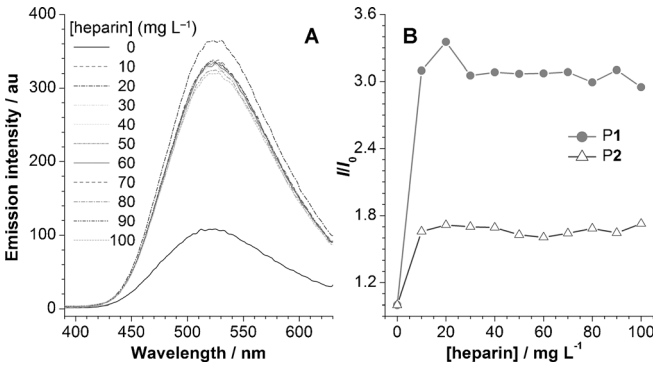

Figure 4. A) Fluorimetric titration of heparin to an aqueous solution of P**1** in water. B) Plot of I/I_0 at 524 (P**1**) and 527 nm (P**2**) versus the heparin concentration. I_0 = emission intensity in the absence of heparin. [P**1**] = [P**2**] = 5 μM; excitation wavelength: 330 nm.

was enhanced approximately threefold along with a 4 nm redshift in the emission maximum. The addition of more heparin does not cause further enhancement in the emission intensity, thereby suggesting that the interaction between P**1** and heparin is saturated at low heparin concentration. Similarly, the aqueous solution of P**2** emits at 527 nm, with intensities increasing by up to 1.6-fold in the presence of heparin (see the Supporting Information and Figure 4B).

In aqueous media, the cationic polymers spontaneously bind to the negatively charged heparin, driven by electrostatic forces. When the polymer strands are bound to the biomolecules, the intramolecular rotation of the TPE units is restricted, which blocks the nonradiative relaxation channels and hence renders the polymers emissive. The free rotation of the TPE phenyl rings in P**2** is somewhat hindered in the aqueous solution owing to the relatively poor water solubility, whereas the free rotation in P**1** is still severe. The P**2** solution thus shows a higher pristine emission intensity I_0 in the absence of heparin and lower relative fluorescent enhancement I/I_0 than P**1**.

Nucleic Acid Detection

Fluorescent probes, the emission of which is activated upon complexation with biomacromolecules such as nucleic acids, are useful biomarkers in genomics.[19] By taking advantage of the "light-up" property, cationic AIE-active CPEs can be employed as probes for the detection of nucleic acids. Calf thymus DNA (ctDNA) and RNA from torula yeast were chosen as models for spectrometric titrations. The PL spectrum of a dilute solution of P**1** in water peaked at 524 nm. The addition of a small amount of ctDNA increased the fluorescence intensity but caused no change in the spectral profile (Figure 5A). The peak intensity increased rapidly at

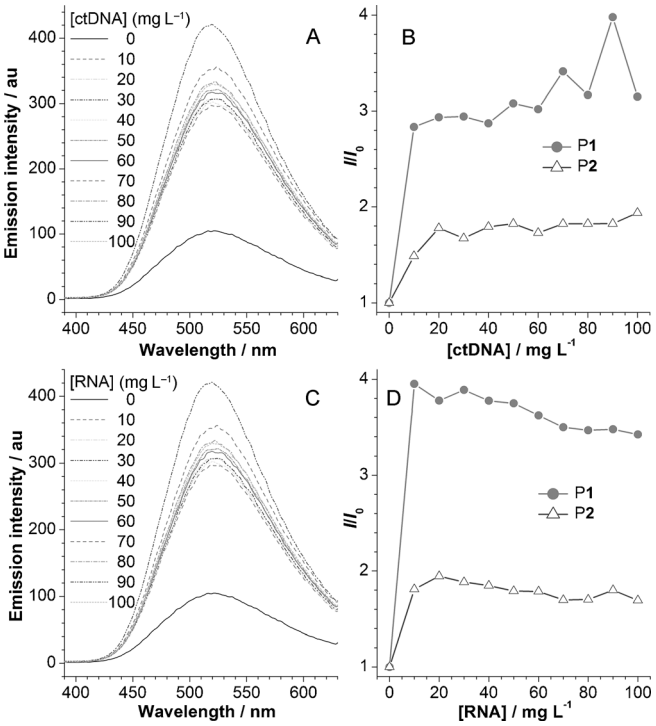

Figure 5. Fluorimetric titration of A) ctDNA and C) RNA to an aqueous solution of P**1** in water. Plot of I/I_0 at 524 (P**1**) and 527 nm (P**2**) versus the B) ctDNA and D) RNA concentration. I_0 = emission intensity in the absence of ctDNA or RNA. [P**1**] = [P**2**] = 5 μM; excitation wavelength = 330 nm.

low ctDNA concentration and gradually became saturated as the ctDNA concentration increased.

The fluorescence intensity of P**1** also becomes higher upon binding to RNA (Figure 5C). The plot of relative PL intensity (I/I_0) versus the RNA concentration shows that the emission rises initially with increasing RNA concentration but decreases slightly when more RNA is present in the aqueous solution. Compared with P**1**, P**2** shows a similar emission enhancement but with a lower sensitivity (see the Supporting Information and Figure 5B,D).

Protein Probe

Besides nucleic acid detection, fluorescent biosensors for protein have also attracted much attention and are of great clinical value for qualitative and quantitative analysis of protein. Bovine serum albumin (BSA) and human serum albumin (HSA) are the most abundant proteins in bovine and human blood plasma, respectively. They play a role in multiple biological functions and are widely studied as protein standards. The detection of BSA and HSA is hence of great importance.[20]

To explore the utility of these CPEs for protein analysis, the emission spectra of P**1** and P**2** in the absence and presence of BSA were measured (see Figure 6A and the Supporting Information). The PL response of their neutral polymer precursor P**5** to the presence of protein was also studied (see the Supporting Information). In the absence of BSA,

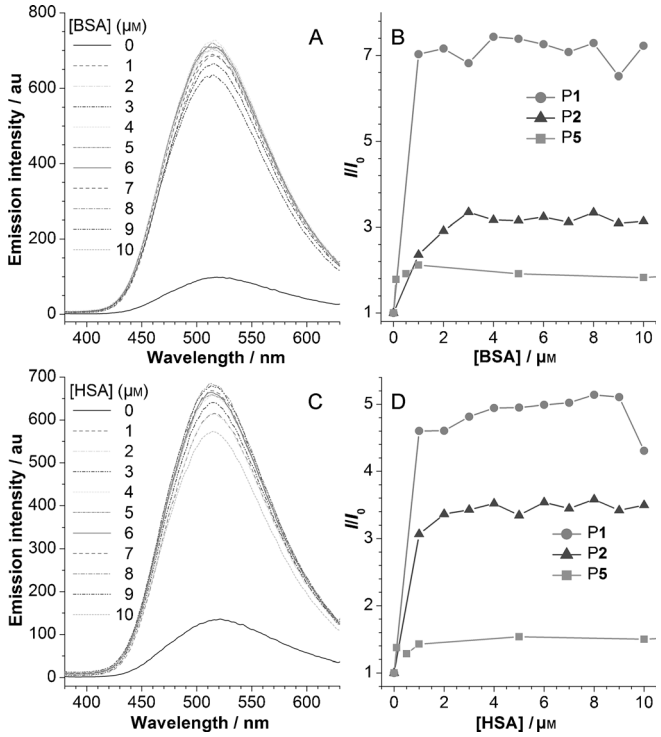

Figure 6. Fluorimetric titration of A) BSA and C) HSA to an aqueous solution of P**1** in water. Plot of I/I_0 at 514 (P**1**), 524 (P**2**), and 534 nm (P**5**) versus the B) BSA or D) HSA concentration. I_0 = emission intensity in the absence of BSA or HSA. [P**1**] = [P**2**] = [P**5**] = 5 μM; excitation wavelength: 330 (P**1** and P**2**) and 367 nm (P**5**).

the aqueous buffer solution (5 μM) of P**1** emitted weakly at 520 nm. The addition of 1 μM BSA aqueous buffer solution resulted in a steep rise in emission intensity by sevenfold, thus demonstrating that P**1** is a promising candidate for trace protein analysis.[21] Unlike heparin and nucleic acid detection, the emission maximum of P**1** shifts to a shorter wavelength of 514 nm when interacting with protein, probably due to the more hydrophobic regions present in the protein molecules, which might cause the CPE chains to adopt a more twisted conformation. The plot of I/I_0 at 514 nm versus the BSA concentration shows a steep upward line at low protein concentration but an almost flat line at high concentration of BSA (Figure 6B). Compound P**2**, which carries triethylammonium groups, shows a merely threefold increase in PL intensity upon binding with BSA because it only dissolves partially in water. P**5** is not soluble in water and emits in DMSO at 536 nm. Its emission intensity increases twofold in the presence of BSA, presumably due to the hydrophobic interaction between the polymer strands and the protein molecules. Quaternization of P**5** furnishes water-soluble polyelectrolytes, which diminishes the emission but enables the polymers to interact with the protein molecules electrostatically. This makes the polymer more emissive and thus results in higher sensitivity upon protein analysis. A similar study was conducted for HSA, and the emission of P**1**, P**2**, and P**5** was enhanced by approximately 5-, 3.5-, and 1.5-fold upon binding with HSA molecules, respectively (see the Supporting Information and Figures 6C, D). The relative fluorescent enhancement for such polyelectrolytes after interaction with biomolecules is generally lower than the water-soluble AIE-active small molecules in the literature.[17c] The TPE units in the polyelectrolytes are knitted together by covalent bonds, which practically restricts their intramolecular rotation and results in an emissive solution. Furthermore, the AEE-active polyelectrolytes with a rigid hydrophobic conjugated polymer backbone do not have as good solubility as the small cationic AIE molecules. The pristine emission intensity I_0 is hence higher for polyelectrolytes than for small compounds, and the relative fluorescent enhancement I/I_0 is the opposite.

To serve as fluorescent visualizers for intracellular cell imaging, it is desirable to prepare AIE materials with longer wavelength emissions because they suffer little interference from cell autofluorescence.[22] With their good water solubility, strong emission efficiency in the aggregated state, and green emission color, the AIE-active CPEs are promising fluorescent staining agents for cell imaging. After 8 h, P**1** selectively stains the cytoplasm of living HeLa cells but not their nuclei (Figure 7). The cells display their normal morphology, which is indicative of the good biocompatibility of P**1**. Endocytosis is believed to be the major route for P**1** to enter the living cells, in which the CPE molecules are first enclosed by the cell membrane to form small vesicles and be internalized by the cells. They are then processed in the endosomes and lysosomes and eventually released to the cytoplasma.[23]

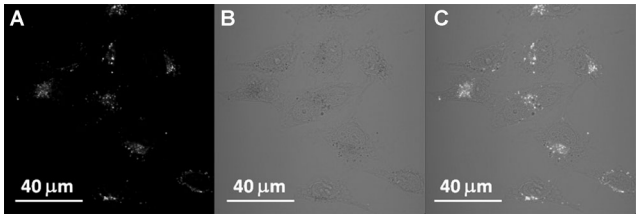

Figure 7. A) Fluorescent, B) bright-field, and C) overlapping images of HeLa cells stained with P**1** for 8 h.

Conclusion

In this paper, TPE-containing polyynes P**5** and P**6** were prepared by Hay–Glaser polycoupling and converted into polyelectrolytes P**1**–P**4** by quaternization with amines. All the polymers were characterized by standard spectroscopic methods with satisfactory results. The neutral polyynes P**5** and P**6** are non- or weakly emissive in THF but become strong emitters when aggregated in poor solvents, thus demonstrating a phenomenon of AIE or AEE. Compound P**1** was found to possess excellent water solubility, whereas P**2**–P**4** are partially soluble in aqueous media. The applications of these fluorescent polyelectrolytes as sensitive, rapidly re-

sponsive, and environmentally stable sensors for biomolecules such as heparin, ctDNA, RNA, BSA, and HSA were explored. The charges and hydrophobic aromatic rings of the polyelectrolytes facilitate their binding with the biomolecules through electrostatic and hydrophobic cooperative interactions, which restrict the intramolecular rotations of their TPE units and leads to a remarkable fluorescence enhancement. They have also proven capable of being used as fluorescent visualizers for intracellular imaging with good biocompatibility and low interference from autofluorescence. The AIE-active conjugated polyelectrolytes are thus promising fluorescent materials for bioprobes and bioimaging. Studies of biologically important processes using these AIE-active fluorescent polyelectrolytes are underway.

Experimental Section

Materials

THF was distilled under normal pressure from sodium benzophenone ketyl under nitrogen immediately prior to use. Compounds **10**, **11**, and **14**; $[Pd(PPh_3)_2Cl_2]$, CuI, PPh_3, zinc powder, $TiCl_4$, tetrabutylammonium fluoride (TBAF), K_2CO_3, trimethylsilylacetylene, copper(I) chloride, TMEDA, *o*-dichlorobenzene, 1,2-dibromoethane, triethylamine, aqueous trimethylamine solution (33%), ethanol, DMSO, and other chemicals and solvents were all purchased from Aldrich and used as received without further purification. Heparin sodium was purchased from Acros. BSA, HSA, ctDNA, and RNA from torula yeast were purchased from Sigma–Aldrich and used as received. Phosphate-buffered saline (PBS) with pH 7.0 was purchased from Merck. Water was purified with a Millipore filtration system. Human cervical cancer HeLa cells were obtained from American Type Culture Collection (ATCC; Rockville, USA). Culture medium and fetal bovine serum (FBS) were purchased from Gibco Laboratories (Grand Island, USA). All the experiments were performed at room temperature.

Instruments

^{1}H NMR spectra were measured with Bruker ARX 400 NMR spectrometers using $CDCl_3$ as solvent and tetramethylsilane (TMS; $\delta = 0$ ppm) as internal standard. UV/Vis absorption spectra were measured with a Milton Roy Spectronic 3000 array spectrophotometer. Photoluminescence spectra were recorded with a Perkin–Elmer LS 55 spectrofluorometer. IR spectra were recorded with a Perkin–Elmer 16 PC FTIR spectrophotometer. Relative number (M_n) and weight-average (M_w) molecular weights and polydispersity indices (PDI or M_w/M_n) of the polymer were estimated with a Waters Associates gel permeation chromatography (GPC) system equipped with RI and UV detectors. THF was used as eluent at a flow rate of 1.0 mL. A set of monodispersed linear polystyrenes that covered the molecular-weight range of 10^3–10^7 was used as standards for the molecular-weight calibration. High-resolution (HR) mass spectra were recorded with a GCT premier CAB048 mass spectrometer operating in MALDI-TOF mode.

Preparation of Aggregates

Stock solution of P**5** and P**6** in THF with a concentration of 0.1 mM was prepared. An aliquot (1 mL) of this stock solution was transferred to a 10 mL volumetric flask. After addition of an appropriate amount of THF, water was dropped slowly under vigorous stirring to furnish a 10 μM THF/water mixture with a specific water fraction. The water content was varied in the range of 0–90 vol%. Absorption and emission spectra of the resulting solutions and aggregates were measured immediately after the sample preparation.

Sample Preparation

Stock solutions of BSA and HSA with a concentration of 100 μM were prepared by dissolving appropriate amounts of protein in PBS (pH 7.0). Heparin, ctDNA, and RNA solutions were prepared in PBS (1.0 mg mL^{-1}). Fluorescence measurement was carried out by adding aliquots (10–100 μL) of heparin (or ctDNA, RNA, BSA, and HSA) solution to the polyelectrolyte solution (1 mL, 5 μM). The mixtures were vortexed prior to the measurements.

Cell Culture and Imaging

HeLa cells were incubated in minimum essential medium (MEM) complemented with 10% FBS, penicillin G (100 U mL^{-1}), and streptomycin (100 μg mL^{-1}) in a 5% CO_2, 90% relative humidity incubator at 37 °C. Compound P**1** was dissolved in PBS (pH 7.4) at a concentration of 5 mg mL^{-1} as a stock solution. HeLa cells were seeded overnight on a cover slip mounted onto a 35 mm Petri dish and then stained with P**1** (50 μg mL^{-1}) for 8 h (by adding stock solution of P**1** (10 μL) to fresh culture medium (990 μL)). After rinsing three times with PBS, the cells were imaged using confocal laser scanning microscopy (CLSM; Carl Zeiss, Germany) at an excitation wavelength of 405 nm and a collection wavelength of 450–600 nm.

Synthesis

The synthetic routes for polyelectrolytes P**1**–P**4** are shown in Schemes 1 and 2. Detailed experimental procedures are given below.

*4,4′-Bis(2-trimethylsilylethynyl)benzophenone (**8**)*

$[PdCl_2(PPh_3)_2]$ (619 mg, 0.88 mmol), CuI (223 mg, 1.17 mmol), PPh_3 (154 mg, 0.59 mmol), **10** (10.0 g, 29.4 mmol), and a solvent mixture of THF/Et_3N (225 mL/75 mL) were added into a 500 mL two-necked round-bottomed flask under an atmosphere of nitrogen. After all the compounds dissolved, (trimethylsilyl)acetylene (16.6 mL, 117.6 mmol) was injected into the flask, and the mixture was stirred at 70 °C for 24 h. The reaction was quenched by adding saturated aqueous NH_4Cl aqueous solution (200 mL). The aqueous phase was extracted with dichloromethane (200 mL, three times). The solvent was removed, and the crude product was purified on a silica gel column by using hexane as eluent. A pale brown solid was obtained in 98% yield. ^{1}H NMR (400 MHz, $CDCl_3$, TMS): $\delta = 7.71$ (d, $J = 8.4$ Hz, 4H), 7.56 (d, $J = 8.4$ Hz, 4H), 0.27 ppm (s, 18H; $Si(CH_3)_3$); IR (KBr): $\tilde{\nu} = 3301$, 3062, 2959, 2899, 2157, 1931, 1655, 1625, 1600, 1552, 1400, 1307, 1288, 1271, 1249, 1219, 1174, 929, 848, 758, 650 cm^{-1}.

*4,4′-Bis(2-bromoethoxy)benzophenone (**9**)*

1,2-Dibromoethane (35.1 g, 186.7 mmol) was added to a mixture of 4,4′-dihydroxybenzophenone (10.0 g, 46.7 mmol) and potassium carbonate (38.7 g, 280.1 mmol) in acetone. The mixture was heated to reflux under stirring overnight. After filtration and solvent evaporation, the crude product was purified by a silica gel column using hexane/ethyl acetate (4:1 v/v) as eluent. Compound **9** was obtained as a white powder in 87% yield. ^{1}H NMR (400 MHz, [D$_6$]DMSO): $\delta = 7.70$ (d, $J = 8.4$ Hz, 4H), 7.10 (d, $J = 8.4$ Hz, 4H), 4.43 (*t*, J=5.2 Hz, 4H), 3.84 ppm (t, $J = 5.2$ Hz, 4H); IR (KBr): $\tilde{\nu} = 3063$, 2948, 2893, 1633, 1603, 1579, 1507, 1308, 1295, 1255, 1226, 1171, 1150, 1024, 854, 841, 763 cm^{-1}; HRMS (MALDI-TOF): m/z calcd: 425.9466 [M^+]; found: 425.9470.

*2,2-Bis[4-(2-bromoethoxy)phenyl]-1,1-bis[4-(2-trimethylsilylethynyl)phenyl]ethene (**7**)*

Compound **8** (2.00 g, 5.34 mmol), **9** (2.28 g, 5.33 mmol), and zinc dust (0.70 g, 10.7 mmol) were placed into a 500 mL two-necked round-bottomed flask with a reflux condenser. The flask was evacuated under vacuum and flushed with dry nitrogen three times. Then THF (150 mL) was added. The mixture was cooled to −78 °C, and $TiCl_4$ (1.71 mL, 5.33 mmol) was added dropwise using a syringe. The mixture was slowly warmed to room temperature, stirred for 0.5 h, and then heated to reflux for 24 h. The reaction was quenched with 10% aqueous K_2CO_3 solution. The resulting mixture was filtered, and the filtrate was extracted with di-

chloromethane three times. The organic layer was washed with water and dried over Na_2SO_4. After solvent evaporation, the residue was purified by silica gel chromatography using petroleum ether/ethyl acetate (4:1 v/v) as eluent. Compound **7** was obtained as a white solid in 29% yield.

*2,2-Bis[4-(2-bromoethoxy)phenyl]-1,1-bis(4-ethynylphenyl)ethene (**5**)*

Compound **7** (2.00 g, 2.59 mmol) and K_2CO_3 (0.36 g, 2.59 mmol) were placed into a 100 mL round-bottomed flask. The reactants were dissolved in methanol (24 mL), THF (15 mL), and $CHCl_3$ (5 mL). The mixture was stirred under nitrogen at room temperature for 3 h, diluted with dichloromethane, and washed three times with water (100 mL). The mixture was extracted three times with dichloromethane (200 mL). The organic layer was then washed twice with brine. The crude product was condensed and purified on a silica gel column using hexane as eluent. A light yellow solid of **5** was obtained in 60% yield. ^{1}H NMR (400 MHz, CD_2Cl_2, TMS): δ = 7.22 (d, J = 8 Hz, 2H), 6.94 (d, J = 8 Hz, 2H), 6.91 (d, J = 7.2 Hz, 2H), 6.65 (d, J = 7.2 Hz, 2H), 4.21 (t, 2H), 3.61 (t, 2H), 3.08 ppm (s, 1H; HC≡); IR (KBr): $\tilde{\nu}$ = 3290 (≡C–H stretching), 3031, 2964, 2925, 2860, 2105 (C≡C stretching), 1603, 1507, 1242, 1175, 1017, 832 cm^{-1}; HRMS (MALDI-TOF): m/z calcd: 624.0300 [M^+]; found: 624.0311.

*4-(2-Bromoethoxy)benzophenone (**13**)*

1,2-Dibromoethane (5.21 g, 27.8 mmol) was added to a mixture of **14** (5.00 g, 25.2 mmol) and potassium carbonate (10.4 g, 75.7 mmol) in acetone. The mixture was heated to reflux under stirring overnight. After filtration and solvent evaporation, the crude product was purified by using a silica gel column with hexane/ethyl acetate (4:1 v/v) as eluent. Compound **13** was obtained as a white powder in 63% yield. ^{1}H NMR (400 MHz, [D$_6$]DMSO): δ = 7.74 (d, J = 8.4 Hz, 2H), 7.68 (d, J = 8.4 Hz, 2H), 7.63 (m, 1H), 7.52 (m, 2H), 7.10 (m, 2H), 4.42 (t, J = 5.2 Hz, 2H), 3.83 ppm (t, J = 5.2 Hz, 2H); IR (KBr): $\tilde{\nu}$ = 3284, 3097, 2975, 2933, 2884, 1651, 1599, 1572, 1508, 1446, 1421, 1476, 1389, 1318, 1255, 1279, 1151, 1175, 1082, 1011, 922, 849, 820, 795, 742, 707, 698 cm^{-1}; HRMS (MALDI-TOF): m/z calcd: 304.0099 [M^+]; found: 304.0089.

*2-[4-(2-Bromoethoxy)phenyl]-2-phenyl-1,1-bis[4-(2-trimethylsilylethynyl)phenyl]ethene (**12**)*

Compound **8** (4.00 g, 10.7 mmol), **13** (3.34 g, 10.9 mmol), and zinc dust (1.40 g, 21.4 mmol) were placed into a 500 mL two-necked round-bottomed flask with a reflux condenser. The flask was evacuated under vacuum and flushed three times with dry nitrogen. THF (200 mL) was then added to dissolve the reactants. The mixture was cooled to −78 °C, and $TiCl_4$ (1.17 mL, 10.7 mmol) was added dropwise with a syringe. The mixture was slowly warmed to room temperature, stirred for 0.5 h, and then heated to reflux for 24 h. The reaction was then quenched with 10% aqueous K_2CO_3 solution. The resulting mixture was filtered, and the filtrate was extracted with dichloromethane three times. The organic layer was washed with water and dried over Na_2SO_4. After solvent evaporation, the residue was purified by silica gel chromatography using petroleum ether/ethyl acetate (4:1 v/v) as eluent to give **12** as a white solid in 26% yield. ^{1}H NMR (400 MHz, $CDCl_3$, TMS): δ = 7.22 (d, J = 8.4 Hz, 2H), 7.18 (d, J = 8.4 Hz, 2H), 7.10 (m, 3H), 6.99 (m, 2H), 6.94–6.88 (m, 6H), 6.64 (d, J = 8.8 Hz, 2H), 4.22 (t, 2H; CH_2), 3.61 (t, 2H; CH_2), 0.23 (s, 9H; $Si(CH_3)_3$), 0.22 ppm (s, 9H; $Si(CH_3)_3$); IR (KBr): $\tilde{\nu}$ = 3075, 3032, 2959, 2898, 2156 (C≡C stretching), 1605, 1507, 1249, 1176, 1018, 861, 841, 760, 670 cm^{-1}; HRMS (MALDI-TOF): m/z calcd: 646.1723 [M^+]; found: 646.1695.

*2-[4-(2-Bromoethoxy)phenyl)]-2-phenyl-1,1-bis(4-ethynylphenyl)ethene (**6**)*

A solution of **12** in THF (40 mL, 1.80 g, 2.78 mmol) was placed into a 100 mL round-bottomed flask. A solution of tetrabutylammonium fluoride in THF (10 mL, 1 M) was then added. After stirring for 3 h, water (40 mL) was added, and the mixture was extracted with dichloromethane (200 mL, three times). The organic layer was washed twice with brine. The crude product was condensed and purified on a silica gel column using hexane as eluent. A light yellow solid of **6** was obtained in 57% yield. ^{1}H NMR (400 MHz, CD_2Cl_2, TMS): δ = 7.22 (m, 4H), 7.11 (m, 3H), 7.01–6.90 (m, 8H), 6.65 (d, J = 8.8 Hz, 2H), 4.23 (t, 2H), 3.61 (t, 2H), 3.06 (s, 1H; HC≡), 3.04 ppm (s, 1H; HC≡); IR (KBr): $\tilde{\nu}$ = 3290 (≡C–H stretching), 3046, 3031, 2960, 2929, 2861, 2107 (C≡C stretching), 1603, 1506, 1290, 1243, 1174, 836, 823, 760 cm^{-1}; HRMS (MALDI-TOF): m/z calcd: 502.0932 [M^+]; found: 502.0933.

Polymerization

The polymerization reaction and manipulation were carried out in an open atmosphere. Typical experimental procedures for the polymerization are given below.

*Polymer P**5***

CuCl (0.4 mg, 0.004 mmol), TMEDA (1.7 mg, 0.015 mmol), and *o*-dichlorobenzene (2 mL) were placed into a test tube equipped with a magnetic stir bar. The catalyst mixture was bubbled with a slow steam of compressed air and stirred at 50 °C for 15 min. Monomer **5** (120 mg, 0.19 mmol) was dissolved in *o*-dichlorobenzene (1 mL) and then added dropwise into the catalyst mixture. After stirring at room temperature for 5 h, the polymerization was terminated by dropping the reaction mixture into methanol (300 mL) acidified with HCl solution (1 mL, 37%). The polymer precipitate was filtered by a Gooch crucible, washed with methanol and hexane, and dried under vacuum overnight at room temperature. A yellow powder was obtained in 99% yield. M_w: 14900; M_w/M_n: 1.91; ^{1}H NMR (400 MHz, CD_2Cl_2, TMS): δ = 7.22 (m, 2H), 6.92 (m, 4H), 6.66 (m, 2H), 4.22 (m, 2H), 3.61 ppm (m, 2H); IR (KBr): $\tilde{\nu}$ = 3287, 3030, 2965, 2926, 2857, 2204 (C≡C–C≡C stretching), 2141 (C≡C–C≡C stretching), 1602, 1574, 1505, 1241, 1173, 1016, 830 cm^{-1}.

*Polymer P**1***

A 250 mL flask with a magnetic stir bar was charged with P**5** (50 mg) in THF (67 mL). Aqueous trimethylamine solution (12 mL, 33%) was added to this solution. The mixture was heated to reflux and stirred for 3 d. After removal of THF, excess amounts of trimethylamine, and water, a yellow powder was obtained in 61% yield. ^{1}H NMR (400 MHz, [D$_6$]DMSO): δ = 7.48, 7.37, 7.10–6.92, 4.49, 3.86, 3.27 ppm; IR (KBr): $\tilde{\nu}$ = 3030, 2958, 2872, 2210 (C≡C–C≡C stretching), 2143 (C≡C–C≡C stretching), 1633, 1603, 1508, 1482, 1241, 1177, 952, 833 cm^{-1}.

*Polymer P**2***

A 250 mL flask with a magnetic stir bar was charged with P**5** (50 mg) in THF (67 mL). Triethylamine (6 mL) was added to the solution. The mixture was then heated to reflux and stirred for 3 d. During this period, water (5 mL) was added at regular time intervals. After evaporation of THF, excess amounts of triethylamine, and water, a yellow powder was obtained in 90% yield. ^{1}H NMR (400 MHz, [D$_6$]DMSO): δ = 7.47, 7.37, 7.09, 7.03, 6.97, 6.87, 6.76, 4.32, 3.86, 3.10, 1.26 ppm; IR (KBr): $\tilde{\nu}$ = 3032, 2935, 2974, 2677, 2209 (C≡C–C≡C stretching), 2143 (C≡C–C≡C stretching), 1603, 1507, 1242, 1174, 1016, 831, 808 cm^{-1}.

*Polymer P**6***

CuCl (0.7 mg, 0.007 mmol), TMEDA (2.8 mg, 0.024 mmol), and *o*-dichlorobenzene (3 mL) were placed into a test tube equipped with a magnetic stir bar. The catalyst mixture was bubbled with a slow steam of compressed air and stirred in an oil bath at 50 °C for 15 min. Monomer **6** (161 mg, 0.32 mmol) was dissolved in *o*-dichlorobenzene (2 mL) and then added dropwise into the catalyst mixture. After stirring at room temperature for 5 h, the polymerization was terminated by dropping the reaction mixture into methanol (300 mL) acidified with HCl solution (1 mL, 37%). The polymer precipitate was filtered by a Gooch crucible, washed with methanol and hexane, and dried under vacuum overnight. A yellow powder was obtained in 91% yield. M_w: 38900; M_w/M_n: 3.85; ^{1}H NMR (400 MHz, $CDCl_3$, TMS): δ = 7.20 (m, 4H), 7.12 (m, 3H), 7.00–6.90 (m, 8H), 6.65 (m, 2H), 4.22 (m, 2H), 3.61 ppm (m, 2H); IR (KBr): $\tilde{\nu}$ = 3030, 2962, 2928, 2204 (C≡C–C≡C stretching), 2142 (C≡C–C≡C stretching), 1601, 1505, 1241, 1174, 1016, 834, 816, 670 cm^{-1}.

Polymer P3

A 250 mL flask with a magnetic stir bar was charged with P**6** (60 mg) in THF (100 mL). Aqueous trimethylamine solution (10 mL, 33%) was added to this solution. The mixture was heated to reflux and stirred for 3 d. After removal of THF, excess amounts of trimethylamine, and water, a yellow powder was obtained in 65% yield. ^{1}H NMR (400 MHz, [D$_6$]DMSO): δ = 7.47, 7.27, 7.07, 6.92, 4.48, 3.95, 3.84 ppm; IR (KBr): $\tilde{\nu}$ = 3031, 2957, 2871, 2207 (C≡C–C≡C stretching), 2143 (C≡C–C≡C stretching), 1633, 1601, 1507, 1481, 1466, 1238, 835, 815, 757, 701 cm^{-1}.

Polymer P4

A 50 mL flask with a magnetic stir bar was charged with P**6** (64 mg) dissolved in THF (20 mL). Triethylamine (10 mL) and water (1 mL) were added to this solution. The mixture was heated to reflux and stirred for 3 d. During this period, water (2 mL) was added at regular time intervals. After removal of THF, excess amounts of triethylamine, and water, a yellow powder was obtained in 84% yield. ^{1}H NMR (400 MHz, [D$_6$]DMSO): δ = 7.46, 7.26, 7.08, 6.89, 6.65, 4.35, 3.86, 3.61, 1.34 ppm; IR (KBr): $\tilde{\nu}$ = 3029, 2964, 2933, 2739, 2677, 2201 (C≡C–C≡C stretching), 2141 (C≡C–C≡C stretching), 1601, 1506, 1261, 1240, 1017, 1033, 834, 806, 700 cm^{-1}.

Acknowledgements

This work was partially supported by the National Basic Research Program of China (973 Program; 2013CB834701), the RPC and SRFI Grants of HKUST (RPC11SC09 and SRFI11SC03PG), the Research Grants Council of Hong Kong (602212, HKUST2/CRF/10 and N_HKUST620/11), and the University Grants Committee of HK (AoE/P-03/08). B.Z.T. is grateful for the support of the Guangdong Innovative Research Team Program (201101C0105067115).

[1] a) A. P. F. Turner, *Chem. Soc. Rev.* **2013**, *42*, 3184–3196; b) J. Tamayo, P. M. Kosaka, J. J. Ruz, A. S. Paulo, M. Calleja, *Chem. Soc. Rev.* **2013**, *42*, 1287–1311; c) K. Saha, S. S. Agasti, C. Kim, X. Li, V. M. Rotello, *Chem. Rev.* **2012**, *112*, 2739–2779; d) P. C. Ray, *Chem. Rev.* **2010**, *110*, 5332–5365; e) F. Feng, F. He, L. An, S. Wang, Y. Li, D. Zhu, *Adv. Mater.* **2008**, *20*, 2959–2964.

[2] a) R. P. Haugland, *Handbook of Fluorescent Probes and Research Chemicals* (Ed.: M. T. Z. Spence), Molecular Probes, Inc. **1996**; b) K. E. Achyuthan, T. S. Bergstedt, L. Chen, R. M. Jones, S. Kumaraswamy, S. A. Kushon, K. D. Ley, L. Lu, D. McBranch, H. Mukundan, F. Rininsland, X. Shi, W. Xia, D. G. Whitten, *J. Mater. Chem.* **2005**, *15*, 2648–2656; c) M. M. Bradford, *Anal. Biochem.* **1976**, *72*, 248–254; d) O. H. Lowry, N. J. Rosebrough, A. L. Farr, R. J. Randall, *J. Biol. Chem.* **1951**, *193*, 265–275.

[3] a) M. J. Whitcombe, I. Chianella, L. Larcombe, S. A. Piletsky, J. Noble, R. Porter, A. Horgan, *Chem. Soc. Rev.* **2011**, *40*, 1547–1571; b) H, Shi, R. T. K. Kwok, J. Liu, B. Xing, B. Z. Tang, B. Liu, *J. Am. Chem. Soc.* **2012**, *134*, 17972–17981; c) B. N. G. Giepmans, S. R. Adams, M. H. Ellisman, R. Y. Tsien, *Science* **2006**, *312*, 217–224; d) C. A. Royer, *Chem. Rev.* **2006**, *106*, 1769–1784; e) Y. Suzuki, K. Yokoyama, *J. Am. Chem. Soc.* **2005**, *127*, 17799–17802; f) D. Matulis, C. G. Baumann, V. A. Bloomfield, R. E. Lovrien, *Biopolymers* **1999**, *49*, 451–458.

[4] a) A. P. Alivisatos, W. Gu, C. Larabell, *Annu. Rev. Biomed. Eng.* **2005**, *7*, 55–76; b) I. L. Medintz, H. T. Uyeda, E. R. Goldman, H. Mattoussi, *Nat. Mater.* **2005**, *4*, 435–446; c) M. De, P. S. Ghosh, V. M. Rotello, *Adv. Mater.* **2008**, *20*, 4225–4241.

[5] a) Y. Zhang, Y. Li, X. P. Yan, *Anal. Chem.* **2009**, *81*, 5001–5007; b) T. Jamieson, R. Bakhshi, D. Petrova, R. Pocock, M. Imani, A. M. Seifalian, *Biomaterials* **2007**, *28*, 4717–4732; c) B. Dubertret, P. Skourides, D. J. Norris, V. Noireaux, A. H. Brivanlou, A. Libchaber, *Science* **2002**, *298*, 1759–1762; d) N. L. Rosi, C. A. Mirkin, *Chem. Rev.* **2005**, *105*, 1547–1562; e) H. Ow, D. R. Larson, M. Srivastava, B. A. Baird, W. W. Webb, U. Wiesnert, *Nano Lett.* **2005**, *5*, 113–117; f) N. Johnsson, K. Johnsson, *ACS Chem. Biol.* **2007**, *2*, 31–38; g) M. Sameiro, T. Gonçalves, *Chem. Rev.* **2009**, *109*, 190–212.

[6] a) S. M. Yarmoluk, D. V. Kryvorotenko, A. O. Balanda, M. Y. Losytskyy, V. B. Kovalska, *Dyes Pigm.* **2001**, *51*, 41–49; b) A. Hawe, M. Sutter, W. Jiskoot, *Pharm. Res.* **2008**, *25*, 1487–1499; c) I. Eryazici, C. N. Moorefield, G. R. Newkome, *Chem. Rev.* **2008**, *108*, 1834–1895; d) M. H. Keefe, K. D. Benkstein, J. T. Hupp, *Coord. Chem. Rev.* **2000**, *205*, 201–228.

[7] a) B. Liu, G. C. Bazan, *Conjugated Polyelectrolytes*, Wiley-VCH, Weinheim, **2013**; b) K. Li, B. Liu, *Polym. Chem.* **2010**, *1*, 252–259; c) P. S. Heeger, A. J. Heeger, *Proc. Natl. Acad. Sci. USA* **1999**, *96*, 12219–12221; d) Q. Zhou, T. M. Swager, *J. Am. Chem. Soc.* **1995**, *117*, 7017–7018; e) M. R. Pinto, K. S. Schanze, *Proc. Natl. Acad. Sci. USA* **2004**, *101*, 7505–7510; f) Z. Yao, X. Feng, C. Li, G. Shi, *Chem. Commun.* **2009**, 5886–5888.

[8] a) C. Zhu, L. Liu, Q. Yang, F. Lv, S. Wang, *Chem. Rev.* **2012**, *112*, 4687–4735; b) S. W. Thomas, G. D. Joly, T. M. Swager, *Chem. Rev.* **2007**, *107*, 1339–1386; c) D. Wang, X. Gong, P. S. Heeger, F. Rininsland, G. C. Bazan, A. J. Heeger, *Proc. Natl. Acad. Sci. USA* **2002**, *99*, 49–53; d) L. Chen, D. W. McBranch, H. L. Wang, R. Helgeson, F. Wudl, D. G. Whitten, *Proc. Natl. Acad. Sci. USA* **1999**, *96*, 12287–12292; e) B. S. Gaylord, A. J. Heeger, G. C. Bazan, *Proc. Natl. Acad. Sci. USA* **2002**, *99*, 10954–10957; f) X. Duan, S. Wang, Z. Li, *Chem. Commun.* **2008**, 1302–1304; g) M. B. Abérem, A. Najari, H. A. Ho, J. F. Gravel, P. Nobert, D. Boudreau, M. Leclerc, *Adv. Mater.* **2006**, *18*, 2703–2707; h) K. P. R. Nilsson, O. Inganas, *Nat. Mater.* **2003**, *2*, 419–424.

[9] a) J. N. Wilson, Y. Wang, J. J. Lavigne, U. H. F. Bunz, *Chem. Commun.* **2003**, 1626–1627; b) T. L. Nelson, C. O'Sullivan, N. T. Greene, M. S. Maynor, J. J. Lavigne, *J. Am. Chem. Soc.* **2006**, *128*, 5640–5641.

[10] B. S. Gaylord, A. J. Heeger, G. C. Bazan, *J. Am. Chem. Soc.* **2003**, *125*, 896–900.

[11] a) S. A. Kushon, K. D. Ley, K. Bradford, R. M. Jones, D. McBranch, D. Whitten, *Langmuir* **2002**, *18*, 7245–7249; b) B. S. Gaylord, S. Wang, A. J. Heeger, G. C. Bazan, *J. Am. Chem. Soc.* **2001**, *123*, 6417–6418.

[12] a) D. T. McQuade, A. E. Pullen, T. M. Swager, *Chem. Rev.* **2000**, *100*, 2537–2574; b) D. T. McQuade, A. H. Hegedus, T. M. Swager, *J. Am. Chem. Soc.* **2000**, *122*, 12389–12390.

[13] a) S. Wang, G. C. Bazan, *Chem. Commun.* **2004**, 2508–2509; b) J. J. Lavigne, D. L. Broughton, J. N. Wilson, B. Erdogan, U. H. F. Bunz, *Macromolecules* **2003**, *36*, 7409–7412; c) C. Y. Tan, M. R. Pinto, K. S. Schanze, *Chem. Commun.* **2002**, 446–447.

[14] J. B. Birks, *Photophysics of Aromatic Molecules*, Wiley, London, **1970**.

[15] a) Y. Hong, J. W. Y. Lam, B. Z. Tang, *Chem. Soc. Rev.* **2011**, *40*, 5361–5388; b) Y. Hong, J. W. Y. Lam, B. Z. Tang, *Chem. Commun.* **2009**, 4332–4353.

[16] a) Z. Li, Y. Q. Dong, J. W. Y. Lam, J. Sun, A. Qin, M. Häussler, Y. P. Dong, H. H. Y. Sung, I. D. Williams, H. S. Kwok, B. Z. Tang, *Adv. Funct. Mater.* **2009**, *19*, 905–917; b) C. X. Yuan, X. T. Tao, L. Wang, J. X. Yang, M. H. Jiang, *J. Phys. Chem. C* **2009**, *113*, 6809–6814; c) M. Zhao, M. Wang, H. Liu, D. Liu, G. Zhang, D. Zhang, D. Zhu, *Langmuir* **2009**, *25*, 676–678; d) M. Wang, D. Zhang, G. Zhang, D. Zhu, *Chem. Commun.* **2008**, 4469–4471.

[17] a) X. Xu, J. Li, Q. Li, J. Huang, Y. Dong, Y. Hong, J. Yan, J. Qin, Z. Li, B. Z. Tang, *Chem. Eur. J.* **2012**, *18*, 7278–7286; b) H. Tong, Y. Hong, Y. Dong, M. Häussler, Z. Li, J. W. Y. Lam, Y. Dong, H. H. Y. Sung, I. D. Williams, B. Z. Tang, *J. Phys. Chem. B* **2007**, *111*, 11817–11823; c) Y. Hong, M. Häussler, J. W. Y. Lam, Z. Li, K. K. Sin, Y. Dong, H. Tong, J. Liu, A. Qin, R. Renneberg, B. Z. Tang, *Chem. Eur. J.* **2008**, *14*, 6428–6437; d) M. Wang, X. Gu, G. Zhang, D. Zhang, D. Zhu, *Anal. Chem.* **2009**, *81*, 4444–4449; e) M. Wang, D. Zhang, G. Zhang, Y. Tang, S. Wang, D. Zhu, *Anal. Chem.* **2008**, *80*, 6443–6448.

[18] S. H. Bai, F. Ahsan, *J. Pharm. Sci.* **2010**, *99*, 4554–4564.

[19] a) R. P. Haugland, *Handbook of Fluorescent Probes and Research Chemicals Molecular Probes Leiden*, **2002**; b) P. Prentø, *Biotech. Histochem.* **2001**, *76*, 137–161; c) G. T. Hirons, J. J. Fawcett, H. A. Crissman, *Cytometry* **1994**, *15*, 129–140; d) M. D. Dutton, R. J. Varhol, D. G. Dixon, *Anal. Biochem.* **1995**, *230*, 353–355; e) G. Malojčić, I. Piantanida, M. Marinić, M. Žinić, M. Marjanović, M. Kralj, K. Pavelić, H. J. Schneider, *Org. Biomol. Chem.* **2005**, *3*, 4373–4381.

[20] a) T. Peters, *Adv. Protein Chem.* **1985**, *37*, 161–245; b) B. D. Rose, *Pathophysiology of Renal Disease*, McGraw Hill, New York, **1987**; c) A. W. Martinez, S. T. Phillips, M. J. Butte, G. M. Whitesides, *Angew. Chem.* **2007**, *119*, 1340–1342; *Angew. Chem. Int. Ed.* **2007**, *46*, 1318–1320.

[21] W. Z. Yuan, H. Zhao, X. Y. Shen, F. Mahtab, J. W. Y. Lam, J. Z. Sun, B. Z. Tang, *Macromolecules* **2009**, *42*, 9400–9411.

[22] a) T. Wang, Y. Cai, Z. Wang, E. Guan, D. Yu, A. Qin, J. Sun, B. Z. Tang, C. Gao, *Macromol. Rapid Commun.* **2012**, *33*, 1584–1589; b) M. Li, Y. Hong, Z. Wang, S. Chen, M. Gao, R. T. Kwok, W. Qin, J. W. Lam, Q. Zheng, B. Z. Tang, *Macromol. Rapid Commun.* **2013**, DOI: 10.1002/marc.201200760.

[23] a) M. Mahmoudi, K. Azadmanesh, M. A. Shokrgozar, W. S. Journeay, S. Laurent, *Chem. Rev.* **2011**, *111*, 3407–3432; b) S. D. Conner, S. L. Schmid, *Nature* **2003**, *422*, 37–44.

Received: April 11, 2013
Published online: July 10, 2013